Ceramics International xxx (xxxx) xxx–xxx

Contents lists available at ScienceDirect

Ceramics International

journal homepage: www.elsevier.com/locate/ceramint

Temperature stability and high-Qf of low temperature firing Mg_2SiO_4–Li_2TiO_3 microwave dielectric ceramics

Yuanming Lai, Caiyun Hong, Lichuan Jin, Xiaoli Tang, Huaiwu Zhang, Xin Huang, Jie Li, Hua Su*

State Key Laboratory of Electronic Thin Films and Integrated Devices, University of Electronic Science and Technology of China, Chengdu 610054, China

ARTICLE INFO

Keywords:
Microwave dielectric ceramic
Temperature stability
High-Qf value
Low temperature firing

ABSTRACT

In this work, a series of low-temperature-firing $(1-x)Mg_2SiO_4$–xLi_2TiO_3–8 wt% LiF (x = 35–85 wt%) microwave dielectric ceramics was prepared through conventional solid state reaction. X-ray diffraction (XRD) and X-ray photoelectron spectroscopy (XPS) analyses showed that the Li_2TiO_3 phase was transformed into cubic phase $LiTiO_2$ phase and secondary phase Li_2TiSiO_5. Partial substitution of Mg^{2+} ions for Ti^{3+} ions or Li^+Ti^{3+} ions increased the cell volume of the $LiTiO_2$ phase. The dense microstructures were obtained in low Li_2TiO_3 content ($x \leq 65$ wt%) samples sintered at 900 °C, whereas the small quantity of pores presented in high Li_2TiO_3 content ($x \geq 75$ wt%) samples sintered at 900 °C and low Li_2TiO_3 content (x = 45 wt%) sintered at 850 and 950 °C. Samples at x = 45 wt% under sintering at 900 °C for 4 h showed excellent microwave dielectric properties of ε_r = 10.7, high Q × f = 237,400 GHz and near-zero τ_f = − 3.0 ppm/°C. The ceramic also exhibited excellent chemical compatibility with Ag. Thus, the fabricated material could be a possible candidate for low temperature co-fired ceramic (LTCC) applications.

1. Introduction

LTCC technology plays an important role in microelectronic applications. This technology requires materials with moderate dielectric constant (ε_r), high Q × f values, near-zero temperature coefficients of resonant frequency ($\tau_f \leq \pm$ 10 ppm/°C) and low firing temperature (~ 961 °C to co-fire with Ag) for practical application [1–5]. Forsterite (Mg_2SiO_4) is an important candidate for microwave applications because of its high Q × f value (Q × f = 240,000 GHz) [6–9]. However, Mg_2SiO_4 ceramics require high sintering temperatures (1350–1450 °C) and negative temperature coefficients of resonance frequency (τ_f = − 67 ppm/°C) to satisfy LTCC application requirements [10–12]. Several glass types, such as lithium borosilicate glass, calcium borosilicate and lithium magnesium zinc borosilicate glasses, are used to reduce the sintering temperature of Mg_2SiO_4 ceramics [13–15]. However, these glass additives exhibit the following two disadvantages: (i) deterioration of microwave dielectric properties [13], and (ii) high sintering temperature requirement (1325 °C for 4 h) [14]. LiF is widely used as sintering aid for microwave ceramics because of its low melting point (~ 848 °C) and retention of remarkable microwave properties [16–20]. According to dielectric complex rules, $CaTiO_3$ and TiO_2 are widely utilized to adjust the τ_f value to zero because of their large positive τ_f of approximately + 800 and + 430 ppm/°C, respectively. But additives of $CaTiO_3$ and TiO_2 can deteriorate dielectric properties [16,21].

The rock salt-type Li_2TiO_3 has attracted considerable attention in microwave dielectric ceramics because of its positive τ_f value, relatively high Q×f value and low sintering temperature [22,23]. However, pure Li_2TiO_3 ceramics with high densification is very difficult to obtain by conventional solid-state method because of porous microstructures and microcracks formed through lithium evaporation and order–disorder phase transition at high temperatures [23–26]. Several approaches have been employed to improve the densification of Li_2TiO_3 ceramics; such approaches include the use of nanosized particles and sintering aids [23,27,28]. Nevertheless, adjustment of the negative τ_f of microwave dielectric ceramics by using Li_2TiO_3 has been rarely reported.

In this work, Mg_2SiO_4 and Li_2TiO_3 composite was obtained by solid phase reaction. The Mg_2SiO_4 and Li_2TiO_3 composites were added with LiF to decrease the sintering temperature. The temperature stability, high-Qf and low-temperature firing of Mg_2SiO_4–Li_2TiO_3 microwave dielectric ceramics were assessed. XRD patterns, XPS spectra, SEM images and Vector Network Analyzer were used to analyze phase composition, microstructure, microwave dielectric properties and chemically compatible with Ag electrode material.

2. Experimental procedure

Mg_2SiO_4 and Li_2TiO_3 ceramics were prepared through solid-state ceramic route. Analytically pure MgO, TiO_2, Li_2CO_3(Shanghai Aladdin

* Corresponding author.
E-mail address: uestcsh77@163.com (H. Su).

http://dx.doi.org/10.1016/j.ceramint.2017.08.192
Received 6 August 2017; Received in revised form 14 August 2017; Accepted 29 August 2017

Biological Technology Co., LTD) and SiO_2 (Sinopharm Chemical Reagent Co., Ltd) were used as starting materials, weighed and wet mixed in distilled water by using zirconia balls in a plastic container for 4 h. The slurry of Mg_2SiO_4 and Li_2TiO_3 was dried and calcined in alumina crucibles at 1350 °C and 850 °C, respectively, for 4 h. The calcined powders were mixed in accordance with the (1-x) Mg_2SiO_4–xLi_2TiO_3–8 wt% LiF (x = 35, 45, 55, 65, 75 and 85 wt%) and ground into fine particles. The samples were then pressed under a uniaxial pressure of 10 MPa into cylindrical disks with 12 mm diameter and 4–5 mm height. Sintering was carried out at temperatures between 850 and 950 °C for 4 h.

The crystalline phase of the ceramics was confirmed using PANalytical X'Pert PRO with Cu K_α radiation (λ = 1.54 Å) at room temperature. The XRD patterns were measured in the 2θ angle range between 10° and 120° with a step of 0.02° and a time per step of 1.0 s. Structural refinements were conducted through Rietveld method using FullProf software. The titanium XPS spectra of x = 45 wt% sintered at 900 °C were recorded with a Kratos XSAM800 spectrometer with monochromatic Al Kα radiation. The microstructures and morphology of the sintered samples were analysed by a scanning electron microscope (SEM) (JSM-7001F; JEOL, Japan) at an accelerating voltage of 20 kV. In order to analyze distribution of element, EDS mapping of x = 45 wt% sintered at 900 °C were also recorded. The density of each sample was measured at room temperature by the Archimedes method using distilled water as the buoyancy liquid. Microwave dielectric properties were assessed by a Vector Network Analyzer (N5230, Agilent Technologies, USA). The relative dielectric constants (ε_r), quality factor ($Q \times f$) and temperature coefficient of resonance frequency (τ_f) of the samples were determined through Hakki–Coleman dielectric resonator method.

3. Results and discussion

The XRD patterns of the (1-x)Mg_2SiO_4–xLi_2TiO_3–8 wt% LiF (x = 35, 45, 55, 65, 75 and 85 wt%) ceramics are shown in Fig. 1. Notably, the main phases include Mg_2SiO_4 (ICDD no. #04–0768), $LiTiO_2$ (ICDD no. #16-0223) and Li_2TiSiO_5 (ICDD no. #82-1955) with increasing x. It is well known that Li_2TiO_3 phase in three modifications: the metastable cubic α-Li_2TiO_3, ordered monoclinic β-Li_2TiO_3 and disordered cubic γ-Li_2TiO_3. α-Li_2TiO_3 phase transforms to the monoclinic β-Li_2TiO_3 at 300 °C and, after which the reversible transition of the β-Li_2TiO_3 to γ-Li_2TiO_3 occurs at 1150–1215 °C. As low Li_2TiO_3 content, the Mg_2SiO_4 additive lead to transformation of Li_2TiO_3 phase into a cubic $LiTiO_2$ phase. Similar changes were obtained for the Li_2TiO_3 ceramics, along with the excess MgO, ZnO and NiO (> 30 wt%) [24–26]. Moreover, since the LiF has a face centered cubic rock salt structure which is

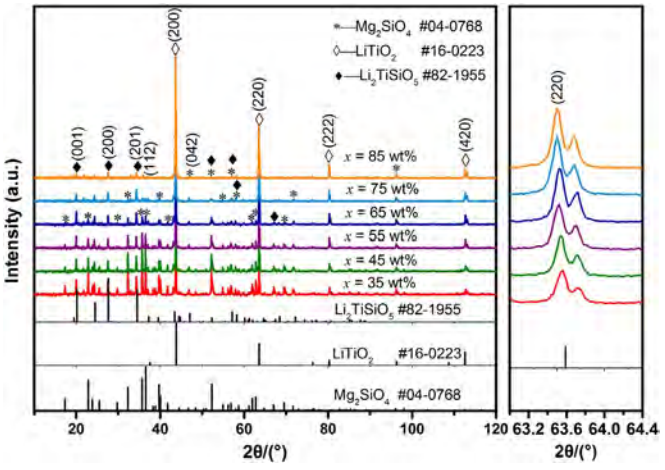

Fig. 1. The XRD patterns of the(1-x)Mg_2SiO_4–xLi_2TiO_3–8 wt% LiF ceramic sintered at 900 °C for 4 h.

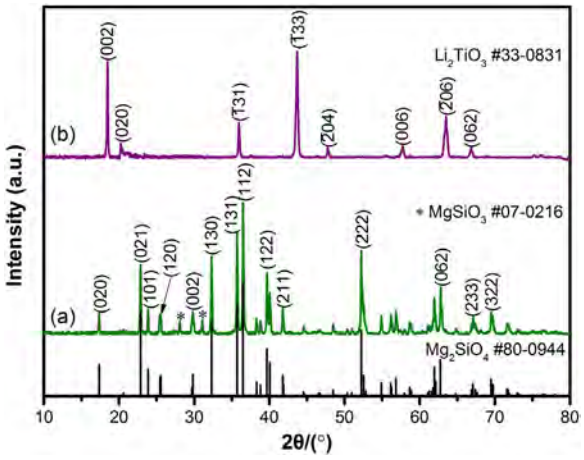

Fig. 2. The XRD patterns of Mg_2SiO_4 (a) and Li_2TiO_3 (b) calcined at 1350 °C and 850 °C, respectively.

similar with that of Li_2TiO_3 (superstructure with edge-sharing cation oxygen octahedral), solid solutions between Li_2TiO_3 and part of LiF can be formed [29]. In the case of high LiF content (8 wt%), a slight amounts of excess Li^+ ions and F^- ions were derived from LiF. These ions enter into Li_2TiO_3 lattice result in Li_2TiO_3 phase present disordered cubic structure ($LiTiO_2$). This can be a main reason the Li_2TiO_3 phase also transform into a cubic $LiTiO_2$ phase with high Li_2TiO_3 content. Similar results were obtained for the (1-x)Li_2TiO_3–xLiF ceramics (when $0.15 \le x \le 0.4$) [30]. In addition, the diffraction peaks of $LiTiO_2$ at the lattice plane were inclined toward the lower diffraction angles. This pattern indicates that the unit cell volumes can increase with increasing x because of the substitution of a larger Mg^{2+} (R = 0.72 Å) for a smaller Ti^{3+} (R = 0.67 Å) or Li^+Ti^{3+} (R_{av} = 0.715 Å), and the replacement mechanism could be proposed as $2Ti^{3+} \leftarrow 3Mg^{2+}$ or $Li^+Ti^{3+} \leftarrow 2Mg^{2+}$ [24]. Moreover, the $MgSiO_3$ phase was detected in calcined powder of Mg_2SiO_4 (Fig. 2(a)). But the $MgSiO_3$ phase unexpectedly disappeared when Mg_2SiO_4 calcined power was sintered with Li_2TiO_3 and LiF. Thus, it can be deduced that the Li_2TiSiO_5 phase may be produced as a result of chemical reaction between $MgSiO_3$ and Li_2TiO_3 phases:

$$Li_2TiO_3 + 2MgSiO_3 \rightarrow Li_2TiSiO_5 + Mg_2SiO_4$$

The Li_2TiSiO_5 phase were also found between Mg_2SiO_4 and TiO_2 phases with LiF in the previous report [16]. The impure phase may deteriorate the dielectric properties. Furthermore, the phase-containing F ions were not detected by XRD when 8 wt% LiF was added. This result may be due to two main reasons. First, partial substitution of O^{2-} ions by F^- ions may have occurred. Second, the LiF may have formed an amorphous phase because the sintering temperature exceeded the compound's melting point (848 °C). Previous research has indicated that the solid solubility limit of F^- in Li_2TiO_3 is about 4 wt%, and when LiF > 6 wt%, a large extent of liquid phase during sintering process inhibit the entrance or occupation of Li^+ and F^- in the Li_2TiO_3 lattice [23,30]. In this work, both of these are likely to really happen because of the LiF content up to 8 wt%. In addition, the EDS elemental mapping analysis of x = 45 wt% ceramic sintered at 900 °C for 4 h are plotted in Fig. 3. It is obvious that F element is uneven distributions in the samples, and partial segregations in some specific regions can be observed.

To obtain the structure, lattice parameter and unit cell volume, the whole XRD pattern was refined using the Fullprof program [31]. Such refinement involved constraining within the orthorhombic, cubic and tetragonal structural models of Mg_2SiO_4 (a = 4.7600 Å, b = 10.2000 Å and c = 5.9900 Å), $LiTiO_2$ ($a = b = c$ = 4.1400 Å) and Li_2TiSiO_5 ($a = b$ = 6.4379 Å, c = 4.4003 Å) with the space groups *Pbnm*, *Fm-3m* and *P4/nmm*, respectively. As representative data, the refined XRD patterns of the x = 45 wt% ceramics are shown in Fig. 4. All the fitted curves

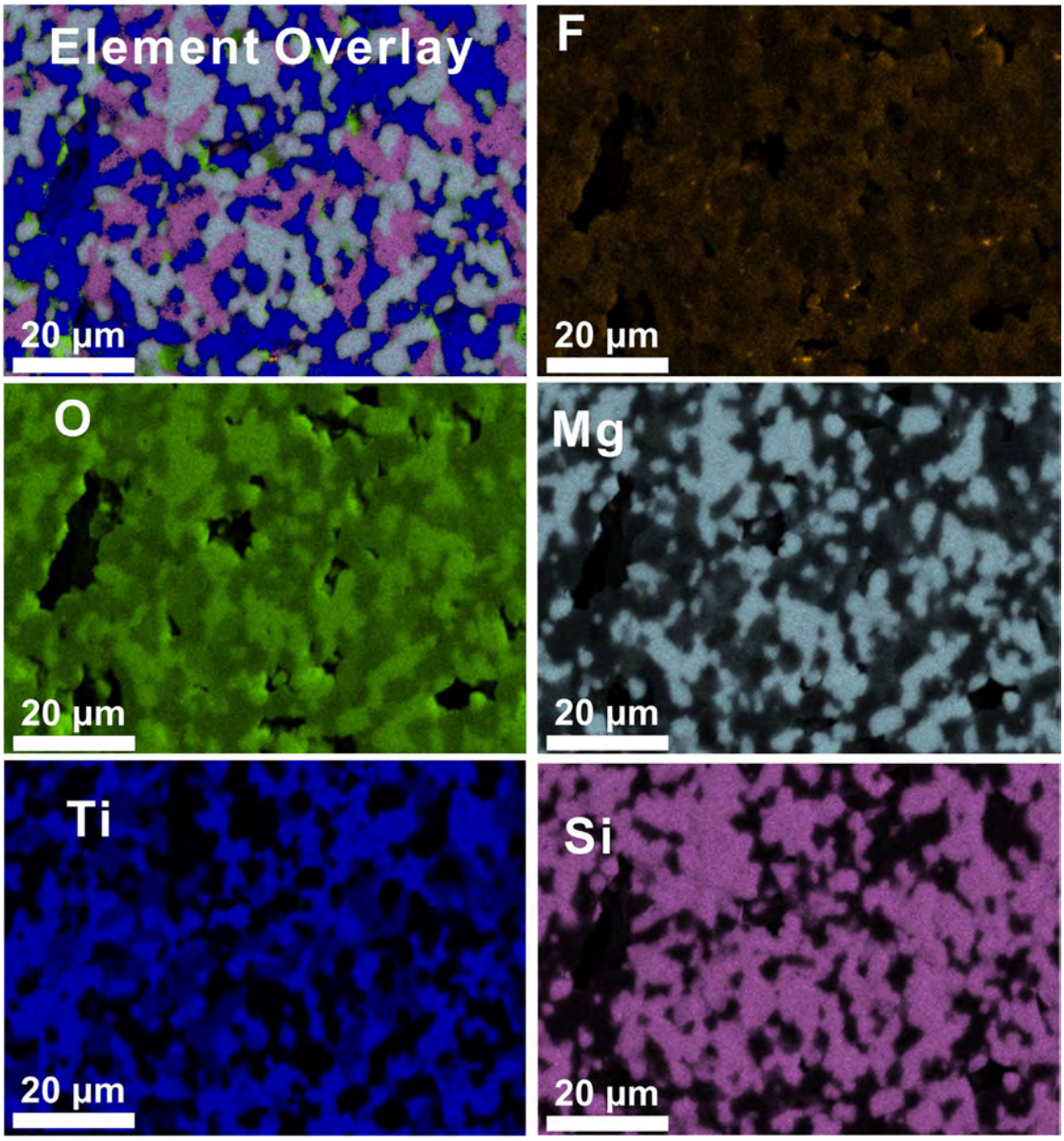

Fig. 3. Elemental mapping of the x = 45 wt% samples sintered at 900 °C for 4 h.

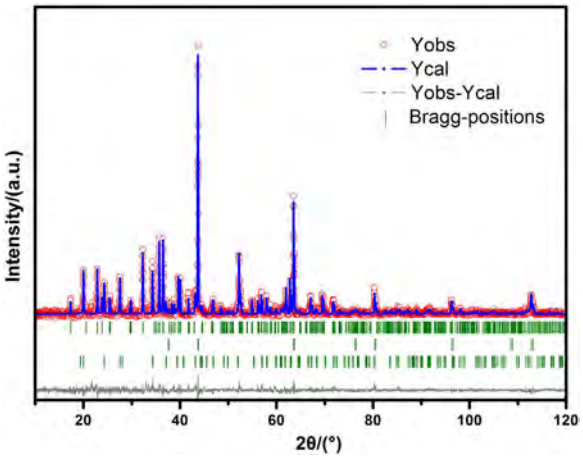

Fig. 4. Rietveld refinements of XRD pattern for x = 45 wt% sintered at 900 °C for 4 h.

match well with the experimental data, and the positions of the Bragg reflections are consistent with the indexed peaks. The refined XRD parameters, lattice constants, R factors and the percentages of the phases are listed in Table 1. The unit cell volumes of $LiTiO_2$ increased with Li_2TiO_3 content addition, consistent with the shift in the diffraction peaks of (220) to lower diffraction angles (Fig. 1).

The x = 45 wt% ceramics sintered at 900 °C were analysed by XPS to investigate the possibility of the valence state of Ti ions. The Ti^{3+} ions in the 457.8 and 463.5 eV energy regions were detected in the x = 45 wt% ceramics (Fig. 5). The ratio of Ti^{3+} to Ti^{4+} was close to 1.5:1 (60.97%: 39.03%), as calculated from the ratio of the peak areas. The results suggest that the Ti^{4+} ions were partially converted into Ti^{3+} ions during the sintering process with Mg_2SiO_4 addition. The Ti^{3+} and Ti^{4+} ions may derive from the $LiTiO_2$ and Li_2TiSiO_5 phases, respectively. According to the refinement results, the ratio of the $LiTiO_2$ phase to the Li_2TiSiO_5 phase was close to 1.1:1 (51.68 mol%:48.32 mol%), which is nearly consistent with the XPS result.

The microstructure of the $(1-x)Mg_2SiO_4$–xLi_2TiO_3–8 wt% LiF ceramics was investigated by SEM (Fig. 6(a)–(g)). In the Fig. 6(a)–(d),

Table 1
Lattice parameters, R factor and the percentages of phases from Rietveld refinement for (1-x)Mg_2SiO_4–xLi_2TiO_3–8 wt% LiF (x = 35, 45, 55, 65, 75 and 85 wt%) ceramics.

		35	45	55	65	75	85
Mg_2SiO_4	a(Å)	4.7558	4.7556	4.7559	4.7554	4.7559	4.6723
	b(Å)	10.1998	10.2001	10.2009	10.2016	10.2085	10.0296
	c(Å)	5.9806	5.9809	5.9811	5.9809	5.9736	6.1924
	V(Å^3)	290.105	290.123	290.169	290.146	290.019	290.182
	wt%	60.96	48.06	32.29	21.18	8.19	0.50
$LiTiO_2$	a(Å)	4.1347	4.1350	4.1362	4.1366	4.1379	4.1380
	V(Å^3)	70.688	70.700	70.762	70.783	70.849	70.855
	wt%	15.03	24.21	39.30	49.24	65.07	82.32
Li_2TiSiO_5	a(Å)	6.4595	6.4591	6.4595	6.4580	6.4566	6.4546
	c(Å)	4.4268	4.4252	4.4245	4.4251	4.4258	4.4204
	V(Å^3)	184.707	184.617	184.614	184.554	184.501	184.158
	wt%	24.02	27.73	28.41	29.58	26.74	17.18
	R_p(%)	9.41	8.87	8.49	8.93	8.75	8.81
	R_{wp}(%)	12.6	11.8	11.3	12.0	11.9	12.1
	R_{exp}(%)	11.44	11.87	12.12	12.36	12.58	12.69
	χ^2	1.41	1.16	0.999	1.11	1.03	1.02

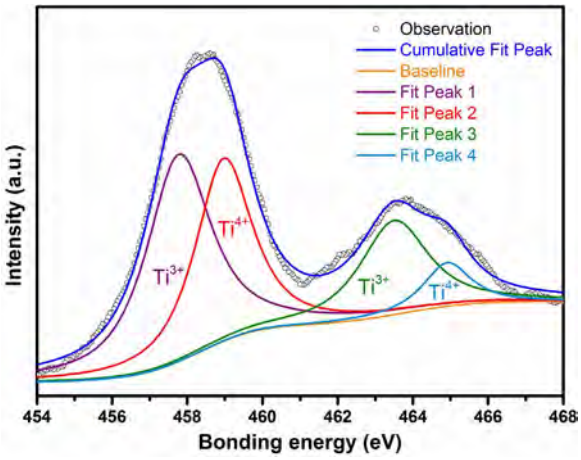

Fig. 5. XPS spectra of Ti 2p for the x = x = 45 wt% samples sintered at 900 °C for 4 h.

the microstructures are dense with no visible porous structure and microcrack. Previous studies indicated the great difficulty in obtaining pure Li_2TiO_3 ceramics with high densification through the conventional solid-state method. And the porous microstructures were also observed in the Li_2TiO_3 ceramics with MgO, ZnO and NiO in the previous work [24–26]. The liquid phase of LiF, which has formed with the high temperature, can promote the densification of the ceramics. Moreover, volatilization of the Li^+ ions in Li_2TiO_3 can result in pores at high temperature. But a moderate amount of excess Li^+ ions, which were derived from LiF, compensate for the escape of Li^+ ions during sintering. Thus, the moderate excess Li^+ ions can be deduced as the one of the reasons underlying the high densification in this work. Similar results were obtained in the nonstoichiometric $Li_{2+x}TiO_3$ ceramics [27]. A small number of pores (enclosed by the dotted line) were observed at $x \geq 75$ wt% sintered at 900 °C, as well as the grain boundaries are not well revealed (Fig. 6(e) and (f)). On the one hand, the volatilization of large amount of Li^+ ions can lead to appear pores. On the other hand, the very rapid mergence of small subgrains leads to the pore isolation in the large grains because of boundary breakaway. Notably, the grain size enlarged with increasing Li_2TiO_3 content because Li_2TiO_3 ceramics involve a lower sintering temperature than that of Mg_2SiO_4 ceramics sintered at 900 °C. The grain size of the ceramics increased from 1 μm to 5 μm for the $x \leq 55$ wt% samples to about 5–20 μm for the $x \leq$ 85 wt% samples. Compared with microstructure of x = 45 wt% sintered at different temperatures (Fig. 6(b), (g) and (h)), the average grain size of the samples tended to increase with the increase of sintering temperature. Incomplete sintering can caused the small grain size (< 1 μm), which can be observed in Fig. 6(g). In addition, the pores were observed as sintered at 850 and 950 °C whereas the dense microstructure was obtained as sintered at 900 °C. Compared with the sintering at 900 °C, higher sintering temperature (950 °C) might lead to volatilization of Li^+ ions and the lower sintering temperature (850 °C) might give rise to incomplete sintering, which is responsible for the pores.

Fig. 7 presents the bulk density as a function of Li_2TiO_3 content for the samples sintered at different temperatures. The bulk densities increased with increasing Li_2TiO_3 content due to comparative higher of theoretical density of Li_2TiO_3 (3.42 g/cm^3) than that of Mg_2SiO_4 (3.21 g/cm^3). Samples sintered at 900 °C exhibited the highest bulk density because the pores present sintered at 850 and 950 °C (Fig. 6(b), (g) and (h)).

Fig. 8 displays the ε_r values of $(1-x)Mg_2SiO_4$–xLi_2TiO_3–8 wt%LiF ceramics as a function of Li_2TiO_3 content. The ε_r show virtually the same values and indicate that the ceramics possess the same phase composition and similar densification at different sintering temperature. In addition, the ε_r linearly increased from 9.5 for x = 35 wt% to a maximum of about 16.5 at x = 85 wt% because of the ε_r values of 6.8 and 22 for Mg_2SiO_4 and Li_2TiO_3, respectively, at microwave frequencies.

The Q × f values of the $(1-x)Mg_2SiO_4$–xLi_2TiO_3–8 wt% LiF ceramics as a function of Li_2TiO_3 content are presented in Fig. 9. The Q × f values of the $(1-x)Mg_2SiO_4$–xLi_2TiO_3–8 wt% LiF ceramics decreased with increasing Li_2TiO_3 content, except in x = 75 wt%. In general, the Q × f values depended on the lattice vibrational modes, lattice defect, ordering structure, secondary phases and inner stress. The optimum Q × f values were also obtained during sintering at 900 °C with the same Li_2TiO_3 contents. This result was significantly associated with the trend in microstructure (excepting in x = 75 wt%) (Fig. 6). Moreover, except in x = 75 wt%, the decrease in Mg_2SiO_4 content may have led to the initial decrease in Q × f values because of the larger Q × f values of the Mg_2SiO_4 phase than that of the $LiTiO_2$ phase [12,24]. At x = 75 wt%, this observation shows the great improvement in Q × f value relative to that of the pure Li_2TiO_3 phase (Q × f ~ 1,5525 GHz) [23,24,28]. Similar results were obtained in 20 mol% MgO and ZnO-doped Li_2TiO_3 ceramics [24,25]. The partial segregation of Mg^{2+} ions, which resulted in the stabilisation of the ordering-induced domain boundaries for the Li_2TiO_3 phase, were responsible for the great improvement in Q × f value [24].

Fig. 10 demonstrates the temperature coefficients of resonant frequency (τ_f) of $(1-x)Mg_2SiO_4$–xLi_2TiO_3–8 wt% LiF ceramics with different x values sintered at 850–950 °C for 4 h. The τ_f values exhibited nonlinear behaviour as a function of x values. However, such values demonstrated the same trends under sintering at different

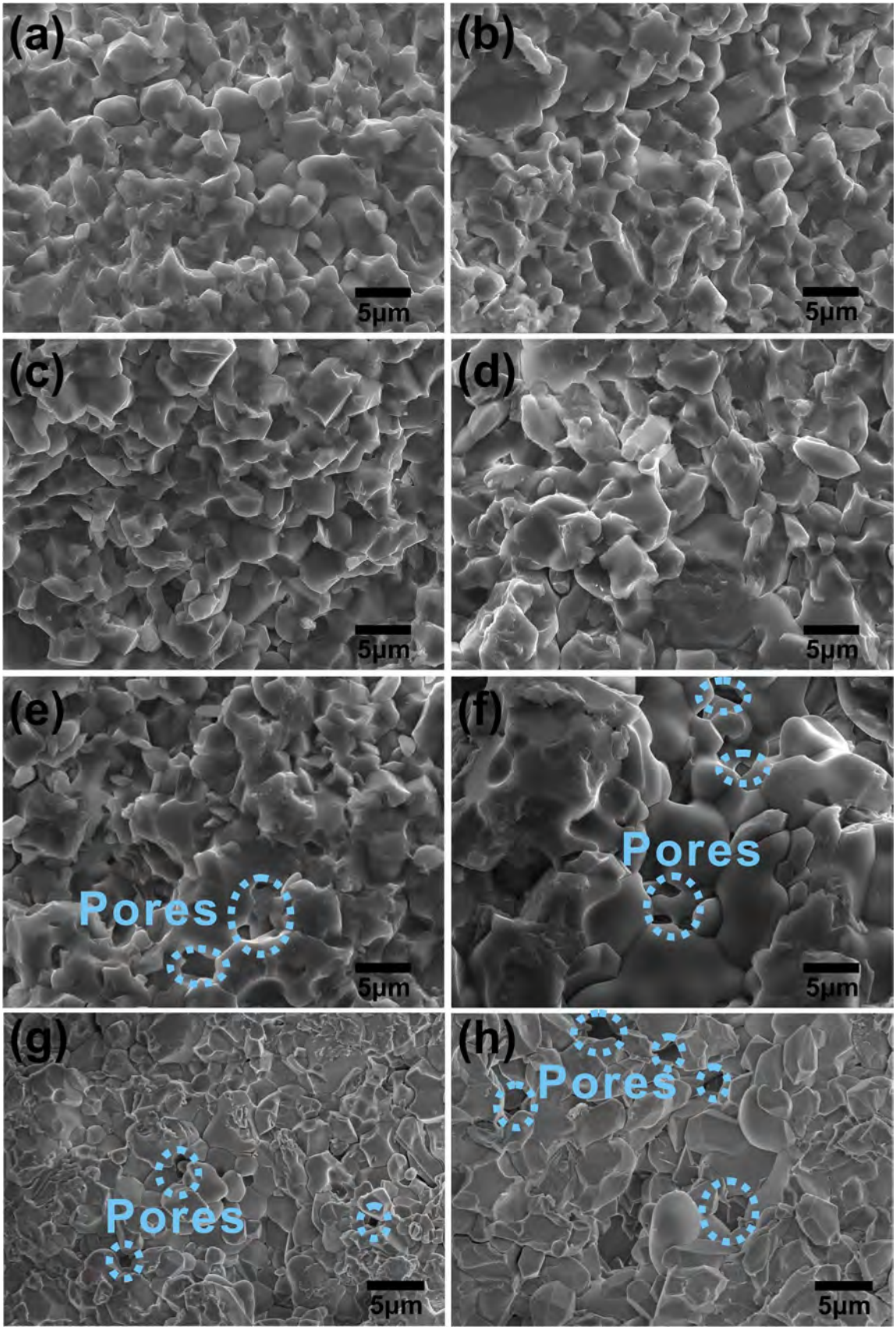

Fig. 6. SEM micrographs of the samples sintered at 900 °C for 4 h with (a) $x = 35$ wt%, (b) $x = 45$ wt%, (c) $x = 55$ wt%, (d) $x = 65$ wt%, (e) $x = 75$ wt% and (f) $x = 85$ wt% together with the SEM micrographs of the $x = 45$ wt% samples sintered at (h) 850 °C and (f) 950 °C for 4 h.

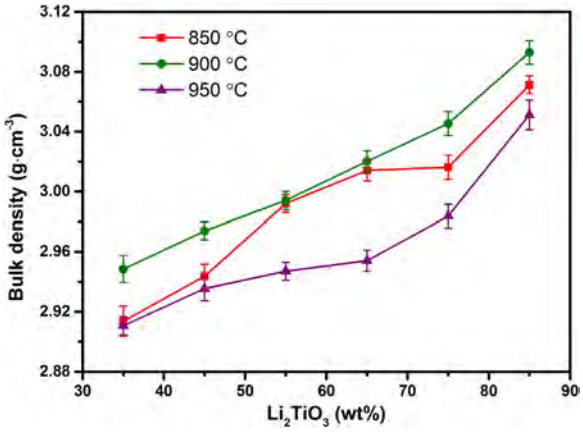

Fig. 7. The bulk density as a function of Li_2TiO_3 content for the samples sintered at different temperatures.

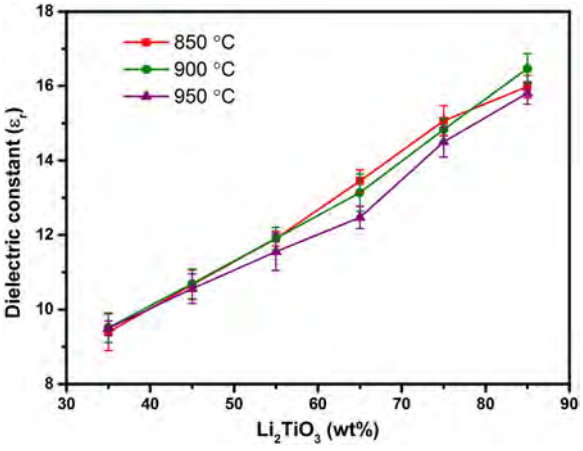

Fig. 8. The dielectric constants of (1-*x*)Mg_2SiO_4–*x*Li_2TiO_3–8 wt% LiF ceramics sintered at different temperature.

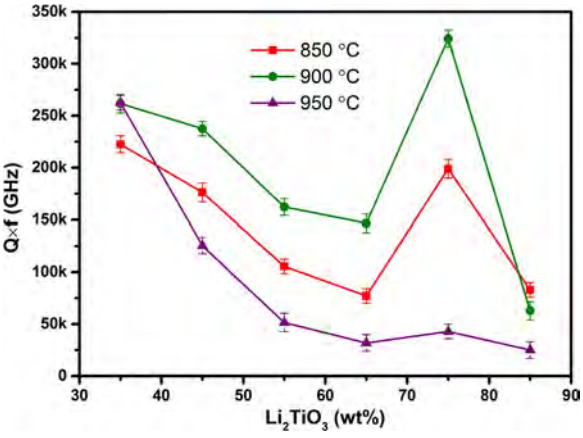

Fig. 9. The Q × f of (1-*x*)Mg_2SiO_4–*x*Li_2TiO_3–8 wt% LiF ceramics sintered at different temperature.

temperatures. In general, the theoretical τ_f values of the mixture are predicted by the semiempirical linear model based on nominal composition:

$$\tau_f = V_1\tau_{f1} + V_2\tau_{f2}$$

where τ_{f1} and τ_{f2} are the τ_f values of Mg_2SiO_4 and Li_2TiO_3 phases, respectively. The τ_f values of the mixed model linearly increased with increasing *x* values. The difference between the measured and mixed τ_f values can be attributed to the production of a secondary phase during the sintering process. Near-zero τ_f values (− 3.0 ppm/°C) were obtained at x = 45 wt% under sintering at 900 °C, as well as excellent microwave dielectric properties of ε_r = 10.7, and Q × f = 237,400 GHz.

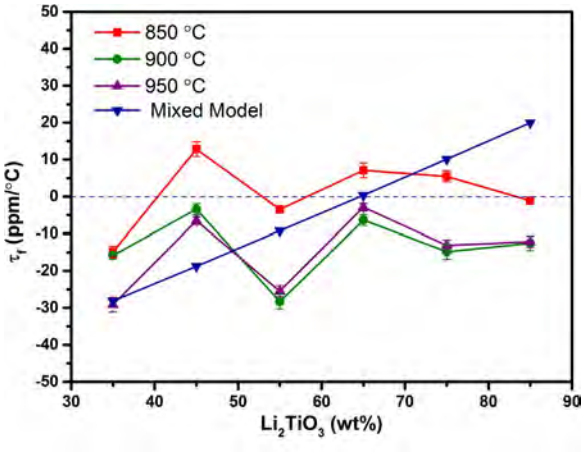

Fig. 10. The τ_f of (1-*x*)Mg_2SiO_4–*x*Li_2TiO_3–8 wt% LiF ceramics sintered at different temperature.

In order to evaluate the chemical compatibility of the (1 − *x*)Mg_2SiO_4–*x*Li_2TiO_3–8 wt% LiF ceramics with electrode materials, 20 wt % Ag was added to x = 45 wt% ceramic. Fig. 11 present the XRD of x = 45 wt% ceramics with 20 wt% Ag. As is seen in Fig. 11, compared with non-Ag ceramic, it can be observed there is no phase of silver compounds presented other than metallic silver (Ag, ICDD #87-0597) phases. It indicated that no reaction occurred between (1 − *x*)Mg_2SiO_4–*x*Li_2TiO_3–8 wt% LiF ceramics and Ag electrodes. Therefore, the (1 − *x*)Mg_2SiO_4–*x*Li_2TiO_3–8 wt% LiF ceramics that exhibited chemical compatibility with Ag could be promising materials for LTCC applications.

4. Conclusions

In this study (1 − *x*)Mg_2SiO_4–*x*Li_2TiO_3–LiF (x = 35, 45, 55, 65, 75 and 85 wt%) microwave dielectric ceramics were prepared using the solid-state reaction method. The specimens could be sintered at 850–950 °C, which is below the melting point of Ag (~ 961 °C). Excellent microwave dielectric properties of ε_r = 10.7, high Q × f = 237,400 GHz and near zero τ_f = − 3.0 ppm/°C were achieved at x = 45 wt% under sintering at 900 °C for 4 h. In addition, these ceramics also exhibited excellent chemical compatibility with Ag. Thus, the

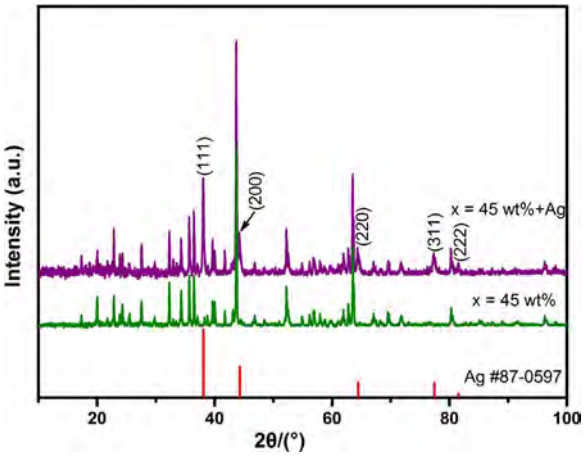

Fig. 11. XRD of x = 45 wt% ceramic with 20 wt% Ag.

fabricated ceramics was considered as a possible candidate for LTCC applications.

Acknowledgements

This work was supported by National Natural Science Foundation of China under Grant nos. 51372031 and 61471096, Science and Technology Department of Sichuan Province 2016JQ0016 and 2016GZ0258, National High-tech R & D Program of China under Grant no. 2015AA034102, National Key Research and Development Plan No. 2016YFA0300801, Fundamental Research Funds for the Central Universities No. A03013023601059.

References

[1] D. Zhou, D. Guo, W.-B. Li, L.-X. Pang, X. Yao, D.-W. Wang, et al., Novel temperature stable high-er microwave dielectrics in the Bi_2O_3–TiO_2–V_2O_5 system, J. Mater. Chem. C 4 (2016) 5357–5362, http://dx.doi.org/10.1039/C6TC01431C.

[2] D. Zhou, L.-X. Pang, Z.-M. Qi, B.-B. Jin, X. Yao, Novel ultra-low temperature co-fired microwave dielectric ceramic at 400 degrees and its chemical compatibility with base metal, Sci. Rep. 4 (2014) 5980, http://dx.doi.org/10.1038/srep05980.

[3] D. Zhou, C.A. Randall, L.X. Pang, H. Wang, J. Guo, G.Q. Zhang, et al., Microwave dielectric properties of Li_2WO_4 ceramic with ultra-low sintering temperature, J. Am. Ceram. Soc. 94 (2011) 348–350, http://dx.doi.org/10.1111/j.1551-2916.2010.04312.x.

[4] H. Chen, H. Su, H. Zhang, T. Zhou, B. Zhang, J. Zhang, et al., Low-temperature sintering and microwave dielectric properties of $(Zn_{1-x}Co_x)_2SiO_4$ ceramics, Ceram. Int. 40 (2014) 14655–14659, http://dx.doi.org/10.1016/j.ceramint.2014.06.053.

[5] L.-X. Pang, D. Zhou, Z. Qi, W. Liu, Z.-X. Yue, I.M. Reaney, Structure-property relations of low sintering temperature scheelite-structured (1-x)$BiVO_4$-x$LaNbO_4$ microwave dielectric ceramics, J. Mater. Chem. C 5 (2017) 2695–2701, http://dx.doi.org/10.1039/C6TC05670A.

[6] T. Tsunooka, M. Androu, Y. Higashida, H. Sugiura, H. Ohsato, Effects of TiO_2 on sinterability and dielectric properties of high-Q forsterite ceramics, J. Eur. Ceram. Soc. 23 (2003) 2573–2578, http://dx.doi.org/10.1016/S0955-2219(03)00177-8.

[7] K.X. Song, X.M. Chen, X.C. Fan, Effects of Mg/Si ratio on microwave dielectric characteristics of forsterite ceramics, J. Am. Ceram. Soc. 90 (2007) 1808–1811, http://dx.doi.org/10.1111/j.1551-2916.2007.01656.x.

[8] K.X. Song, X.M. Chen, C.W. Zheng, Microwave dielectric characteristics of ceramics in Mg_2SiO_4-Zn_2SiO_4 system, Ceram. Int. 34 (2008) 917–920, http://dx.doi.org/10.1016/j.ceramint.2007.09.057.

[9] Y. Chen, X. Dong, R. Liang, J. Li, Y. Wang, Dielectric properties of $Ba_{0.6}Sr_{0.4}TiO_3$-Mg_2SiO_4-MgO composite ceramics, J. Appl. Phys. 98 (2005) 64107, http://dx.doi.org/10.1063/1.2058194.

[10] K.X. Song, X.M. Chen, Phase evolution and microwave dielectric characteristics of Ti-substituted Mg_2SiO_4 forsterite ceramics, Mater. Lett. 62 (2008) 520–522, http://dx.doi.org/10.1016/j.matlet.2007.05.078.

[11] I.-J. Shon, H.-S. Kang, J.-M. Doh, J.-K. Yoon, Rapid synthesis and consolidation of nanostructured Mg_2SiO_4-$MgAl_2O_4$ composites, Mater. Trans. 52 (2011) 2007–2010, http://dx.doi.org/10.2320/matertrans.M2011188.

[12] J. Sugihara, K. Kakimoto, I. Kagomiya, H. Ohsato, Microwave dielectric properties of porous Mg_2SiO_4 filling with TiO_2 prepared by a liquid phase deposition process, J. Eur. Ceram. Soc. 27 (2007) 3105–3108, http://dx.doi.org/10.1016/j.jeurceramsoc.2006.11.032.

[13] T.S. Sasikala, M.N. Suma, P. Mohanan, C. Pavithran, M.T. Sebastian, Forsterite-based ceramic-glass composites for substrate applications in microwave and millimeter wave communications, J. Alloy. Compd. 461 (2008) 555–559, http://dx.doi.org/10.1016/j.jallcom.2007.07.084.

[14] H. Yang, E. Li, C. Sun, S. Duan, Y. Yuan, B.I.N. Tang, The influence of sintering temperature on the microwave dielectric properties of Mg_2SiO_4 ceramics with CaO-B_2O_3-SiO_2 addition, J. Electron. Mater. 46 (2017) 1048–1054, http://dx.doi.org/10.1007/s11664-016-5046-8.

[15] T.S. Sasikala, C. Pavithran, M.T. Sebastian, Effect of lithium magnesium zinc borosilicate glass addition on densification temperature and dielectric properties of Mg_2SiO_4 ceramics, J. Mater. Sci. Electron. 21 (2010) 141–144, http://dx.doi.org/10.1007/s10854-009-9882-7.

[16] J. Ma, T. Yang, Z. Fu, P. Liu, Q. Feng, L. Zhao, Low-fired Mg_2SiO_4-based dielectric ceramics with temperature stable for LTCC applications, J. Alloy. Compd. 695 (2016) 3198–3201, http://dx.doi.org/10.1016/j.jallcom.2016.11.310.

[17] J. Zhang, Z. Yue, Y. Luo, X. Zhang, L. Li, Novel low-firing forsterite-based microwave dielectric for LTCC applications, J. Am. Ceram. Soc. 1124 (2016) 1122–1124, http://dx.doi.org/10.1111/jace.14132.

[18] A. Yokoi, H. Ogawa, A. Kan, H. Ohsato, Y. Higashida, Microwave dielectric properties of $Mg_4Nb_2O_9$-3.0 wt% LiF ceramics prepared with $CaTiO_3$ additions, J. Eur. Ceram. Soc. 25 (2005) 2871–2875, http://dx.doi.org/10.1016/j.jeurceramsoc.2005.03.157.

[19] J. Zhang, Y. Zhou, Z. Yue, Low-temperature sintering and microwave dielectric properties of LiF-doped $CaMg_{1-x}Zn_xSi_2O_6$ ceramics, Ceram. Int. 39 (2013) 2051–2058, http://dx.doi.org/10.1016/j.ceramint.2012.08.058.

[20] A. Yokoi, H. Ogawa, A. Kan, H. Ohsato, Y. Higashida, Use of LiF to achieve a lowtemperature cofired ceramics (LTCC) with low dielectric loss, J. Ceram. Soc. Jpn. 112 (1) (2004) S1633–S1636.

[21] G. Dou, D. Zhou, M. Guo, Low-temperature sintered Mg_2SiO_4–$CaTiO_3$ ceramics with near-zero temperature coefficient of resonant frequency, J. Mater. Sci. Mater. Electron. 24 (2013) 1431–1438, http://dx.doi.org/10.1007/s10854-012-0945-9.

[22] Q. Zeng, W. Li, J. Shi, J. Guo, M. Zuo, W. Wu, A new microwave dielectric ceramic for LTCC applications, J. Am. Ceram. Soc. 89 (2006) 1733–1735, http://dx.doi.org/10.1111/j.1551-2916.2006.00942.x.

[23] J.L. Ma, Z.F. Fu, P. Liu, B. Wang, Y. Li, Microwave dielectric properties of low-fired Li_2TiO_3-MgO ceramics for LTCC applications, Mater. Sci. Eng. B Solid-State Mater. Adv. Technol. 204 (2016) 15–19, http://dx.doi.org/10.1016/j.mseb.2015.10.007.

[24] J.J. Bian, Y.F. Dong, New high Q microwave dielectric ceramics with rock salt structures: (1-x)li_2TiO_3 + xMgO system ($0 \le x \le 0.5$), J. Eur. Ceram. Soc. 30 (2010) 325–330, http://dx.doi.org/10.1016/j.jeurceramsoc.2009.04.030.

[25] C. Huang, Y. Tseng, J. Chen, High-Q dielectrics using ZnO-modified Li_2TiO_3 ceramics for microwave applications, J. Eur. Ceram. Soc. 32 (2012) 3287–3295.

[26] J. Zhang, R. Zuo, Low-temperature fired thermal-stable Li_2TiO_3-NiO microwave dielectric ceramics, J. Mater. Sci. Mater. Electron. 27 (2016) 7962–7968, http://dx.doi.org/10.1007/s10854-016-4789-6.

[27] Y. Hao, Q. Zhang, J. Zhang, C. Xin, H. Yang, Enhanced sintering characteristics and microwave dielectric properties of Li_2TiO_3 due to nano-size and nonstoichiometry effect, J. Mater. Chem. 22 (2012) 23885, http://dx.doi.org/10.1039/c2jm33788f.

[28] J. Liang, W.Z. Lu, J.M. Wu, J.G. Guan, Microwave dielectric properties of Li_2TiO_3 ceramics sintered at low temperatures, Mater. Sci. Eng. B Solid-State Mater. Adv. Technol. 176 (2011) 99–102, http://dx.doi.org/10.1016/j.mseb.2010.09.009.

[29] Y. Hao, H. Yang, G. Chen, Q. Zhang, Microwave dielectric properties of Li_2TiO_3 ceramics doped with LiF for LTCC applications, J. Alloy. Compd. 552 (2013) 173–179, http://dx.doi.org/10.1016/j.jallcom.2012.10.110.

[30] Y. Ding, J. Bian, Structural evolution, sintering behavior and microwave dielectric properties of $(1-x)Li_2TiO_3 + xLiF$ ceramics, Mater. Res. Bull. 48 (2013) 2776–2781, http://dx.doi.org/10.1016/j.materresbull.2013.03.043.

[31] J. Rodríguez-Carvajal, Recent advances in magnetic structure determination by neutron powder diffraction, Phys. B Condens. Matter 192 (1993) 55–69, http://dx.doi.org/10.1016/0921-4526(93)90108-I.